Article

The Journal of Computational Multiphase Flows

The Journal of Computational Multiphase Flows
January-March 2016, Vol. 8(1) 48–60

DOI: 10.1177/1757482X16634198
cmf.sagepub.com
SAGE

Effect of Reynolds number on phase change of water flowing across two heated circular cylinders in tandem arrangement

BK Dhar[1], SK Mahapatra[2], SK Maharana[3] and A Sarkar[1]

Abstract

The situations of fluid flow and heat transfer across an array of cylinders have been quite common in fluid dynamics and, particularly, industry applications. One such situation is flow of water over heated cylinders in a tandem arrangement. The flow of water over heated cylinders faces a phenomenon of phase change from liquid (water) to vapor phase (steam).The mechanism of this phase change is studied through a numerical simulation in this project. The Eulerian model is used in the present simulation method to comprehend the multiphase phenomenon. The effect of Reynolds number on the phase change is studied. The phase change of water in an unsteady flow across cylinders has been prominently affected by Reynolds number. Only critical cases have been discussed in this paper. The volume fraction of water and steam is plotted against the position of flow from inlet to exit of the flow domain that is a channel for a particular flow conditions to demonstrate the phenomenon of heat and mass transfer during the flow of water.

Keywords

Multiphase fluid flow, Eulerian model, tandem arrangement, volume fraction, phase change, Reynolds number

Introduction

The problems of fluid flow and heat transfer phenomena over array of cylinders are quite prominent in fluid dynamics and industry applications.[1,2] These problems give rise to some of the important aspects in fluid dynamics theory such as fluid flow interaction, interferences in flow, vortex dynamics, and a variety of engineering applications such as compact heat exchangers, cooling of electronic equipment, nuclear reactor fuel rods, cooling towers, chimney stacks, offshore structures, hot-wire anemometry, and flow control. The mentioned structures are subjected to air or water flows and therefore experience flow-induced forces which can lead to their failure over a long time. Basically, with respect to the free stream direction, the configuration of two cylinders can be classified as tandem, side-by-side, and staggered arrangements. Quite a few studies on these problems have been carried out analytically, experimentally, and numerically, especially under the configuration of two tandem cylinders for simplicity.

Some of the outstanding research activities in the above field have focused on the effect of spacing between the cylinders on the flow characteristics and heat transfer around them. It was observed that the qualitative nature of the flow depends strongly on the arrangement of cylinders.[1,3,4]

Numerical simulations of flow over a pair of circular cylinders have been carried out by applying different methods that are mainly based on finite element formulation. Mittal et al.[3] have investigated the problem numerically using a stabilized finite element method and reported their study for the Reynolds numbers (Re) of 100 and 1000 in tandem and staggered arrangements for different spacings and concluded that at $Re = 1000$ and $L/D = 2.5$, unlike $Re = 100$, in which the flow converged to initial steady state after some

[1]Department of Mechanical Engineering, Jadavpur University, Kolkata, West Bengal, India
[2]School of Mechanical Sciences, IIT, Bhubaneswar, Jadavpur, India
[3]Department of Aeronautical Engineering, Acharya Institute of Technology, Bangalore, India

Corresponding author:
BK Dhar, Department of Mechanical Engineering, Jadavpur University, Kolkata, West Bengal 700032, India.
Email: dhar.binaya@gmail.com

transience, the shear layers caused instability due to the increased velocity of flow. Increasing the gap to $L/D = 5.5$, the flow at $Re = 100$ showed unsteady behavior. They indicated that the Strouhal numbers that are associated with the vortex shedding of the twin cylinders could take on the same value.

The available experimental investigations and numerical simulations demonstrated rich hydrodynamic phenomena for the problems of fluid flow over double circular cylinders.

In addition to the early experimental investigations, many researchers studied this problem by using numerical simulations. Considering the low Reynolds number $Re = 100$, Ljungkrona et al.[5] reported two flow patterns for the laminar flow over twin tandem circular cylinders. For the large spacing ratio ($L/D > 3.0$), the vortices are observed to be shed from both twin cylinders. However, for small spacing ratios ($L/D < 3.0$), the vortex shedding is observed for only the cylinder downstream, and the vortices in the near wakes of the two cylinders rotate in the same direction, but they are slightly out of phase.

In this respect, wake interaction between two circular cylinders in tandem and side-by-side arrangements was studied experimentally by some researchers such as Zhang and Melbourne,[6] Bearman and Wadcock,[7] Liu et al.,[8] and Ryu et al.[9] In their experimental work, Bearman and Wadcock[7] applied a flow visualization method to study the effect of interference between two circular cylinders in side-by-side arrangement at $Re = 2.5 \times 10^4$. At low Reynolds numbers, Liu et al.[8] employed also the unstructured spectral element method to investigate the flow pattern of two side-by-side cylinders for different spacings.

In the meantime, the flow pattern for tandem arrangement was recently studied numerically by Mahir and Altac,[10] Singha and Sinhamahapatra,[11] Ding et al.,[12] and Kitagawa and Ohta[13] for both laminar and turbulent regimes. Deng et al.[14] performed a numerical study on three-dimensional (3D) effects in the wake of two-fixed tandem cylinders at $Re = 220$. They used the virtual boundary method to apply the no-slip condition. Like two-dimensional (2D) case, they found the critical spacing range for which instability occurred at $3.5 \leq L/D \leq 4$, implying that for $L/D \leq 3.5$, the flow wake maintained a 2D state, while for $L/D \geq 4$, 3D effects appeared in the wake.

As a matter of fact, few numerical works have been done on flow over a pair of cylinders at high Reynolds numbers. One of the most recent significant studies involves 3D simulation of flow over two tandem cylinders at the subcritical $Re = 2.2 \times 10^4$ by Kitagawa and Ohta.[13] They changed the gap from 2D to 4D and analyzed the interference effect and vortex interaction of the two cylinders. Their results showed good agreement with the experimental data at the same Reynolds number. Of noticeable experimental works at subcritical Reynolds numbers, one can mention the studies of Ljungkrona et al.[5] at $Re = 2 \times 10^4$ and Moriya et al.[15] at $Re = 6.5 \times 10^4$. They thoroughly investigated the flow characteristics of two tandem cylinders.

Zdravkovich[16] summarized the drag forces, pressure distribution, velocity profile, vortex shedding frequency, and flow patterns for the twin circular cylinders in a tandem arrangement.

The above literature review has encouraged the authors to contribute towards understanding the phase change phenomenon, while water is flowing over two circular cylinders of equal diameters and in tandem arrangement by changing Reynolds number of the flow.

The fluid flow over a single cylinder is amply covered by much literature in the past and hence this has motivated taking up of a situation where there is more than one cylinder. Before taking up of a problem where two-cylinder arrangement is considered, it is felt that the approach and essence of this research will be incomplete without solving a flow over a single cylinder. To validate a few outcomes of the flow over a single cylinder, leading literature was reviewed and results of laminar flow ($Re = 200$) over a single cylinder is presented here in this paper.

The fluid flow (either laminar or turbulent) over these cylinders with certain heat flux is more relevant as far as the challenges of phase change are concerned. In the present case, it is deemed appropriate to attempt to simulate numerically the phase change phenomenon. This attempt would throw light upon the various challenges and opportunities of phase change from water to steam in a simple case like two-cylinder arrangement in a tandem arrangement. This is kept as one of the objectives for a faster understanding of the physics of phase change.

The impact of Reynolds number on the overall energy and momentum transfer through the fluid flow is noted by volumetric change of water and steam inside the channel. The faster movement of molecules of water and quicker advection signify how two different phases re-orient themselves in terms of volume fractions of each phase.

Physical problem and modeling of trapezoidal cavity receiver

Set up

A sketch of the numerical set up (shown in x–y plane) for two circular cylinders in tandem arrangement with boundary conditions is shown in Figure 1. The necessary dimensions of the fluid domain are expressed in

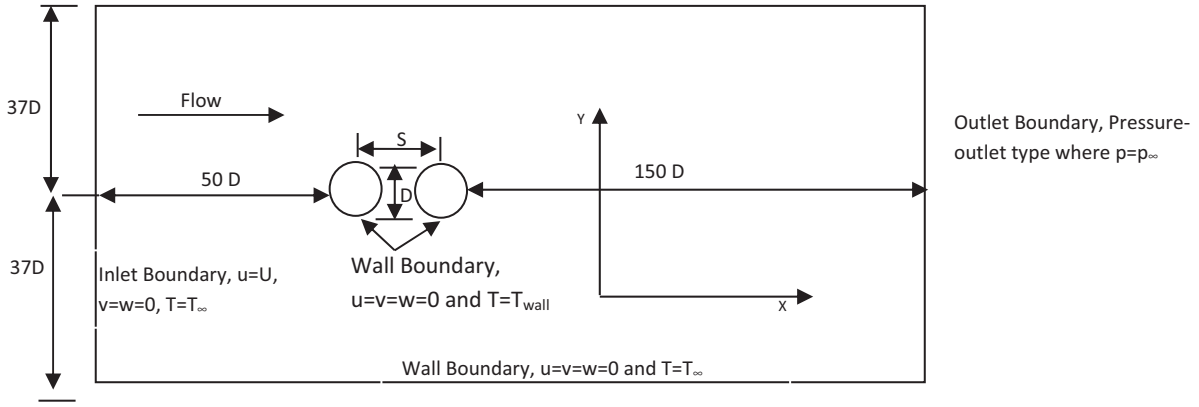

Figure 1. Sketch definition of numerical set up (shown in *x–y* plane) for two circular cylinders in tandem arrangement with boundary conditions.

terms of the diameter (D) of the cylinder. The diameters of both the cylinders are the same. The components of the fluid velocity (U) are u, v in the x-, and y- directions, respectively. Here T is the temperature which has a free stream value at the inlet of the flow (left to right in the flow domain) and it is equal to the wall temperature specified at the boundary of the solid surfaces of both cylinders. Water enters at the left inlet and comes in contact with fixed Cylinder 1 and fixed Cylinder 2 with a distance of 'S' between them.

Mathematical modelling

The Eulerian model has been adopted in the current problem.[16] In this model, a set of $\boldsymbol{n}$ momentum and continuity equations for each phase has been solved. Coupling is achieved through the pressure and interphase exchange coefficients. The manner in which this coupling is handled depends upon the type of phases involved; granular (fluid–solid) flows are handled differently than non-granular (fluid–fluid) flows. For the current problem, coupling has been handled by considering non-granular flows.

The description of multiphase flow as interpenetrating continua incorporates the concept of phasic volume fractions, denoted here by α_q. Volume fractions represent the space occupied by each phase, and the laws of conservation of mass and momentum are satisfied by each phase individually.

The volume of phase 'q' is defined by V_q

$$V_q = \int \alpha_q \mathrm{d}V \tag{1}$$

where

$$\sum_{q=1}^{n} \alpha_q = 1 \tag{2}$$

The effective density of phase q is $\hat{\rho}_{q=\alpha_q \rho_q}$ where ρ_q is the physical density of phase q. The volume fraction equation may be solved either through implicit or explicit time discretization.

The Eulerian multiphase model allows for the modeling of multiple separate, yet interacting phases. A set of conservation equations for momentum, continuity, and (optionally) energy is individually solved for each phase.

The basic set of governing equations used to solve the multiphase flow problem is given below.

The general conservation equations for conservation of mass, conservation of momentum, and energy are presented below

Conservation of mass. The continuity equation for phase q is

$$\frac{\partial}{\partial t}\left(\alpha_q \rho_q\right) + \nabla \cdot \left(\alpha_q \rho_q \vec{v}_q\right) = \sum_{p=1}^{n}\left(\dot{m}_{pq} - \dot{m}_{qp}\right) + S_q \tag{3}$$

where $\vec{v}_q$ is the velocity of phase $\boldsymbol{q}$ and $\dot{\boldsymbol{m}}_{pq}$ characterizes the mass transfer from the $\boldsymbol{p}$th to $\boldsymbol{q}$th phase, and $\dot{\boldsymbol{m}}_{qp}$ characterizes the mass transfer from phase $\boldsymbol{q}$ to phase $\boldsymbol{p}$. The source term $\boldsymbol{S}_q$ on the right-hand side of the above equation is zero, but it can be specified as a constant or user-defined mass source for each phase.

Conservation of momentum. The momentum equation for phase $\boldsymbol{q}$ is

$$\begin{aligned}\frac{\partial}{\partial t}\left(\alpha_q \rho_q \vec{v}_q\right) + \nabla.\left(\alpha_q \rho_q \vec{v}_q \vec{v}_q\right) = &-\alpha_q \nabla p + \nabla.\bar{\bar{\tau}}_{\cdot q} + \alpha_q \rho_q \vec{g} \\ &+ \sum_{p=1}^{n}\left(\vec{R}_{pq} + \dot{m}_{pq}\vec{v}_{pq} - \dot{m}_{qp}\vec{v}_{qp}\right) \\ &+ \left(\vec{F}_q + \vec{F}_{\mathrm{lift},q} + \vec{F}_{vm,q}\right)\end{aligned} \tag{4}$$

where qth phase stress–strain tensor is

$$\bar{\bar{\tau}}_q = \alpha_q \mu_q \left(\nabla \vec{v}_q + \nabla \vec{v}_q^T\right) + \alpha_q \left(\lambda_q - \frac{2}{3}\mu_q\right) \nabla . \vec{v}_q \bar{\bar{I}} \quad (5)$$

Here μ_q and λ_q are the shear and bulk viscosity of phase q, $\vec{F}_q$ is an external body force, $\vec{F}_{lift,q}$ is a lift force, $F_{vm,q}$ is a virtual mass force, $\vec{R}_{pq}$ is an interaction force between phases, and p is the pressure shared by all phases. Then $\vec{v}_{pq}$ is the interphase velocity, defined as follows: If $\dot{m}_{pq}$ (i.e. phase p mass is being transferred to phase q), $\vec{v}_{pq} = \vec{v}_p$; if $\dot{m}_{pq} < 0$ (i.e. phase q mass is being transferred to phase p), $\vec{v}_{pq} = \vec{v}_q$. Likewise, if $\dot{m}_{qp} > 0$ then $\vec{v}_{qp} = \vec{v}_q$, if $\dot{m}_{qp} < 0$ then $\vec{v}_{qp} = \vec{v}_p$.

Equation (4) must be closed with appropriate expressions for the interphase force, $\vec{R}_{pq}$. This force depends on the friction, pressure, cohesion, and other effects and is subject to the conditions that $\vec{R}_{pq} = -\vec{R}_{qp}$ and $\vec{R}_{qq} = 0$

Here a simple interaction term is used stated below

$$\sum_{p=1}^{n} \vec{R}_{pq} = \sum_{p=1}^{n} K_{pq}\left(\vec{v}_p - \vec{v}_q\right) \quad (6)$$

where $K_{pq}\left(= K_{qp}\right)$ is the interphase momentum exchange coefficient.

For fluid–fluid flows, each secondary phase is assumed to form droplets or bubbles. This has an impact on how each of the fluids is assigned to a particular phase. For example, in flows where there are unequal amounts of two fluids, the predominant fluid should be modeled as the primary fluid, since the sparser fluid is more likely to form droplets or bubbles. The exchange coefficient for these types of bubbly, liquid–liquid or gas–liquid mixtures can be written in the following general form

$$K_{pq} = \frac{\alpha_q \alpha_p \rho_p f}{\tau_p} \quad (7)$$

where f is the drag function, is defined differently for the different exchange-coefficient model and τ_p, the "particulate relaxation" time, is defined as

$$\tau_p = \frac{\rho_p d_p^2}{18 \mu_q} \quad (8)$$

where d_p is the diameter of the bubbles or droplet of phase p.

The drag function f is not computed separately in the problem. However, it is given here as a part of the explanation of the basic equations involved in the entire computing work of the project.

Nearly all definitions of f include a drag coefficient (C_D) that is based on the relative Reynolds number. It is this drag function that differs among the exchange-coefficient models.

For all these situations, K_{pq} should tend to zero whenever the primary phase is not present within the domain. To enforce this, the drag function f is always multiplied by the volume fraction of the primary phase q, as is reflected in Equation (7).

The Schiller and Neumann model[17] is the default method, and it is acceptable for general use for all fluid–fluid pairs of phases and hence f is expressed as

$$f = \frac{C_D Re}{24} \quad (9)$$

where

$$C_D = \begin{cases} 24(1 + 0.15 Re 0.678)/Re & Re \le 1000 \\ 0.44 & Re > 1000 \end{cases} \quad (10)$$

and Re is the relative Reynolds number. The relative Reynolds number for the primary phase q and secondary phase p is obtained from

$$\frac{\rho_q |\vec{v}_p - \vec{v}_q| d_p}{\mu_q} \quad (11)$$

Lift forces. For multiphase flows, the effect of lift forces on the secondary phase particles (or droplets or bubbles) is included. These lift forces act on a particle mainly due to velocity gradients in the primary-phase flow field. The lift force will be more significant for larger particles, but for simplified analysis, it can be assumed that the particle diameter is much smaller than the interparticle spacing. Thus, the inclusion of lift forces is not appropriate for closely packed particles or for very small particles.

The lift force acting on a secondary phase p in a primary phase q is computed from Drew and Lahey.[18]

$$\overrightarrow{F}_{lift} = -0.5 \rho_q \alpha_p \left(\vec{v}_p - \vec{v}_q\right) \times \left(\nabla \times \vec{v}_q\right) \quad (12)$$

The lift force $\vec{F}_{lift}$ will be added to the right-hand side of the momentum equation for both phases $\left(\vec{F}_{lift,q} = -\vec{F}_{lift,p}\right)$. In most cases, the lift force is insignificant compared with the drag force, so there is no reason to include this extra term. If the lift force is significant (e.g. if the phases separate quickly), it may be appropriate to include this term. Thus, $\vec{F}_{lift}$ is not included. The lift force and lift coefficient can be specified for each pair of phases, if desired.

The computation of lift force and drag force is computed for the cylinders by the solver. However, the effect of lift force is assumed insignificant compared with the drag force and hence is not included.

Virtual mass force. For multiphase flows, the model includes the "virtual mass effect" that occurs when a secondary phase p accelerates relative to the primary phase q. The inertia of the primary-phase mass encountered by the accelerating particles (or droplets or bubbles) exerts a "virtual mass force" on the particles.[18]

$$\vec{F}_{vm} = 0.5\alpha_p\rho_q\left(\frac{d_q\vec{v}_q}{dt} - \frac{d_q\vec{v}_q}{dt}\right) \tag{13}$$

The term $\frac{d_q}{dt}$ denotes the phase material time derivative of the form

$$\frac{d_q(\emptyset)}{dt} = \frac{\partial(\emptyset)}{\partial t} + (\vec{v}_q \cdot \nabla)\emptyset \tag{14}$$

The virtual mass force $\vec{F}_{vm}$ will be added to the right-hand side of the momentum equation for both phases ($\vec{F}_{vm,q} = -\vec{F}_{vm,p}$). The virtual mass effect is significant when the secondary phase density is much smaller than the primary-phase density. $\vec{F}_{vm}$ is not included.

Virtual mass force is not considered in the current problem because the relative acceleration between the secondary phase (vapor) and the primary phase is neglected.

Conservation of energy. Conservation of energy in Eulerian multiphase applications. The current problem uses this form of the equation

$$\frac{\partial}{\partial t}(\alpha_q\rho_q h_q) + \nabla\cdot(\alpha_q\rho_q\vec{u}_q h_q) = -\alpha_q\frac{\partial p_q}{\partial t} + \bar{\bar{\tau}}_q : \vec{u}_q - \nabla\cdot\vec{q}_q + S_q + \sum_{p=1}^{n}\left(Q_{pq} + \dot{m}_{pq}h_{pq} - \dot{m}_{qp}h_{qp}\right) \tag{15}$$

where h_q is the specific enthalpy of the qth phase, $\vec{q}_q$ is the heat flux, S_q is a source term that includes sources of enthalpy (e.g. due to chemical reaction or radiation), Q_{pq} is the intensity of heat exchange between the pth and qth phases, and h_{pq} is the interphase enthalpy (e.g. the enthalpy of the vapor at the temperature of the droplets, in the case of evaporation). The heat exchange between phases must comply with the local balance conditions $Q_{pq} = -Q_{qp}$ and $Q_{pq} = 0$.

Turbulence models. In comparison with single-phase flows, the number of terms to be modeled in the momentum equations in multiphase flows is large, and this makes the modeling of turbulence in multiphase simulations extremely complex. In the present problem, $k-\epsilon$ models have been employed which are a mixture of the turbulence model. The description of the mixture turbulence model is presented below.

The $k-\epsilon$ mixture turbulence model. The mixture turbulence model is the multiphase turbulence model which has been used in the present computation. It represents the first extension of the single-phase $k-\epsilon$ model, and it is applicable when phases separate, for stratified (or nearly stratified) multiphase flows, and when the density ratio between phases is close to 1. In these cases, using mixture properties and mixture velocities is sufficient to capture the important features of the turbulent flow.

The k and ϵ equations describing this model are as follows

$$\frac{\partial}{\partial t}(\rho_m k) + \nabla\cdot(\rho_m\vec{v}_m k) = \nabla\cdot\left(\frac{\mu_{t,m}}{\sigma_k}\nabla k\right) + G_{k,m} - \rho_m\epsilon \tag{16}$$

and

$$\frac{\partial}{\partial t}(\rho_m\epsilon) + \nabla\cdot(\rho_m\vec{v}_m\epsilon) = \nabla\cdot\left(\frac{\mu_{t,m}}{\sigma_\cdot}\nabla\epsilon\right) + \frac{\epsilon}{k}(C_{1\epsilon}G_{k,m} - C_{2\epsilon}\rho_m\epsilon) \tag{17}$$

where the mixture density ρ_m and velocity $\vec{v}_m$ are computed from

$$\rho_m = \sum_{i=1}^{N}\alpha_i\rho_i \tag{18}$$

and

$$\vec{v}_m = \frac{\sum_{i=1}^{N}\alpha_i\rho_i\vec{v}i}{\sum_{i=1}^{N}\alpha_i\rho_i} \tag{19}$$

The turbulent viscosity, $\mu_{t,m}$ is computed from

$$\mu_{t,m} = \rho_m C_\mu\frac{k^2}{\epsilon} \tag{20}$$

and the production of turbulence kinetic energy, $G_{k,m}$ is computed from

$$G_{k,m} = \mu_{t,m}\left(\nabla\cdot\vec{V}_m + \left(\nabla\vec{V}_m\right)\cdot T\right) : \nabla\vec{V}_m \tag{21}$$

The constants in these equations are given below for the single-phase k–ϵ model. The same constants are used while solving the equations for each phase.

$$C_\mu = 0.09,\quad C_1\varepsilon = 1.44,\quad C_{2\epsilon} = 1.92,\quad \sigma_k = 1.0,\ \sigma_\epsilon = 1.3$$

Boundary conditions

Boundary conditions for the above set up are as follows:

(i) Inlet to the domain: Velocity inlet, $U_\infty = 1$ m/s.
(ii) Outlet from the domain: Gauge pressure outlet, $p = 0$ pascal.
(iii) Wall of the domain: No slip wall boundary (top and bottom).
(iv) Cylinder wall surface: Heat flux, $q'' = 10{,}000\ \mathrm{W/m^2}$ (for both the cylinders).
(v) Cylinder 1: Stationary wall.
(vi) Cylinder 2: Stationary wall.

Solution procedure and mesh independence study

The continuity, momentum, and energy equations are solved as per the Eulerian model for multiphase using Ansys(R) Fluent 12.1 solver.[16] The phase coupled SIMPLE method has been chosen in the solver to compute the flow variables. The turbulent quantities k and ϵ are solved as per the mixture turbulence model. The descriptions of both are given in the above section. The iteration of all the steps ends when the full convergence is achieved. Residual values include the momentum equations for each phase, k and ϵ equations for each phase, and pressure correction residual for continuity equation.

During the heat transfer from the walls of the cylinders to water, which is liquid, it starts to go to a new phase, steam. The mechanism of heat and mass transfer from water to steam is set during the multiphase flow settings. The mass transfer from Phase 1 (water) to Phase 2 (steam) is computed using the unidirectional mass transfer mechanism option in Fluent. Momentum, energy, and turbulence are also transported with the mass that is transferred.

The convergence of the numerical solutions is obtained from the above-mentioned problem using the residuals of the values of variables such as continuity of the flow, velocities of two phases (primary and secondary), and the energy of each phase, turbulent kinetic energy, and its rate of dissipation. In this work, convergence occurs when the values of total residual in all the above-mentioned equations become smaller than 10^{-5}. All these values have reached their acceptable steady solutions during the simulation. The solutions are also independent of the mesh resolution. For the present simulation, initial mesh elements are 306,550 and the convergence of residual error is below the above-mentioned value. The mesh elements are increased to 1.5 times due to finer meshing. The simulation is again carried out and convergence criteria satisfied. The values of all field variables obtained from the two simulations are compared and found to be the same.

Grid quality has been satisfactory after checking the skewness as 0.2 and over all grid quality 0.92 (the highest value is 1.0). The automatic gridding method of the Ansys workbench has optimized the grid density appropriately to fit into flow domain and overall grid quality.

Results and discussion

Verification of the code

First of all, the mean drag coefficient, mean lift coefficient, and Strouhal numbers of the isolated circular cylinder have been compared with those of the other researchers as mentioned in Table 1. The mean drag coefficient versus Re of the flow is plotted in Figure 2. The comparison of the present values of mean drag coefficient with the previously published data is fairly good.

Figure 3 is a plot of Strouhal number which confirms that flow is oscillating and it gives a frequency distribution of vortex shedding from the cylinder. These results are taken for $Re = 200$. The comparison and the validation of the approach have encouraged the authors to continue studying the flow variables when there is a flow over two heated circular cylinders.

Mean drag coefficient, C_D^M, mean lift coefficient C_L^M, and Strouhal number, St, are compared with some of the leading references. From Table 1, it is observed that the computed values of mean drag coefficient, mean lift coefficient, and Strouhal number agree well with the values published by leading researchers in the field.

The spacing between the centers of cylinders is expressed in terms of the diameter, D. The numerical experiments are done at different Reynolds numbers of

Table 1. Comparison of the mean drag coefficient C_D^M, C_L^M and St.

	C_D^M	C_L^A	St
Present	1.41	0.692	0.1902
Ming-Ming et al.[17]	1.337	0.685	0.1955
Rajani et al.[19]	1.3380	0.4276	0.1936
Wang et al.[20]	–	0.71	0.1950
Zhang et al.[21]	1.34	0.66	0.1970
Linnick and Fascl[22]	1.34–1.37	0.71	–
Farrani et al.[23]	1.36–1.39	0.71	–
He et al.[24]	1.36	–	0.1978
Data compiled by Zdravkovich[16]	1.43	–	–
Henderson[25]	1.34–1.37	–	0.1971

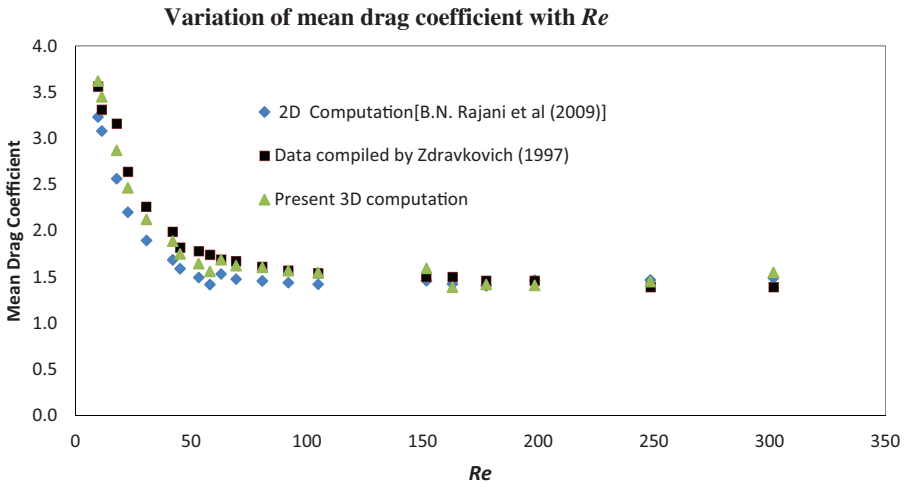

Figure 2. Comparison of mean drag coefficients for various Reynolds numbers for a single circular cylinder.

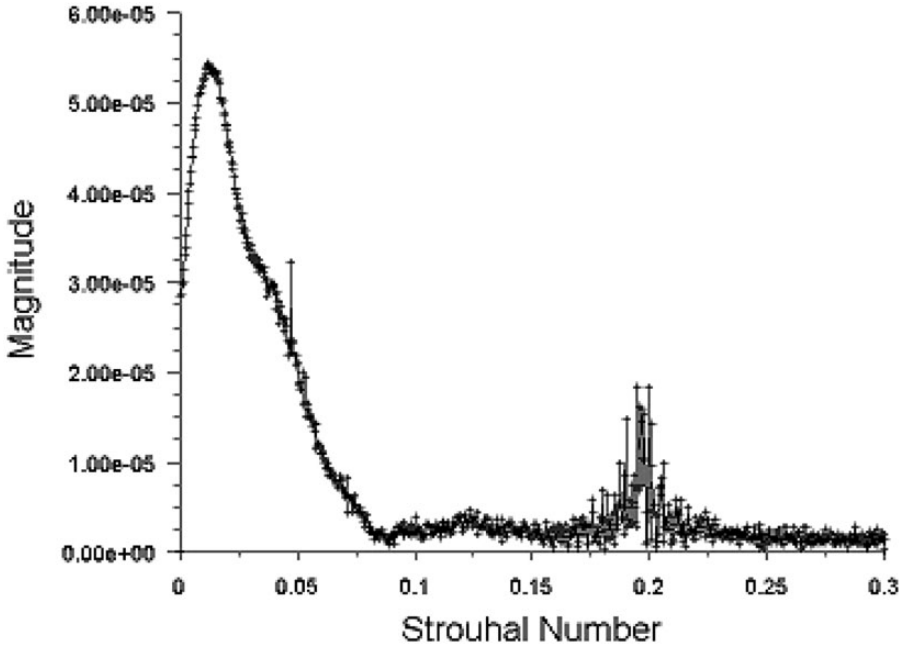

Figure 3. Strouhal number of vortex shedding from the isolated cylinder.

the flow and spacing is kept fixed meter. The study aims to observe the motion of different phases in the wake of the cylinders when there is an interaction between the flows of the cylinders and while the flow becomes non-interacting for a gradual increase of Reynolds number.

Basically two Reynolds numbers are considered in this study for a spacing between the two cylinders. Both the cylinders, having the same diameter and length, are heated and the heat flux is maintained at 10,000 W/m^2. The heated cylinders are kept in a tandem arrangement at two different spacings: 1.5 D and 6 D. At a particular spacing, water is allowed to flow across the cylinders and its phase change is observed. Two values of Re are considered for each spacing. One value of Re is 200 (laminar flow) and the other value is 1.5×10^5 (turbulent flow). The aim of the numerical experiment is to note and analyze the volume fraction of each phase (liquid and vapor) when water flows at a Re over two the heated cylinders kept at a spacing (1.5 D or 6 D). The inlet temperature of the water is 300 K. During the study, it is also noted that the surface heat transfer coefficients of the heated cylinders get affected by the variation of Reynolds number. An empirical correlation ($h = q/\Delta T$) is adopted for the computation of

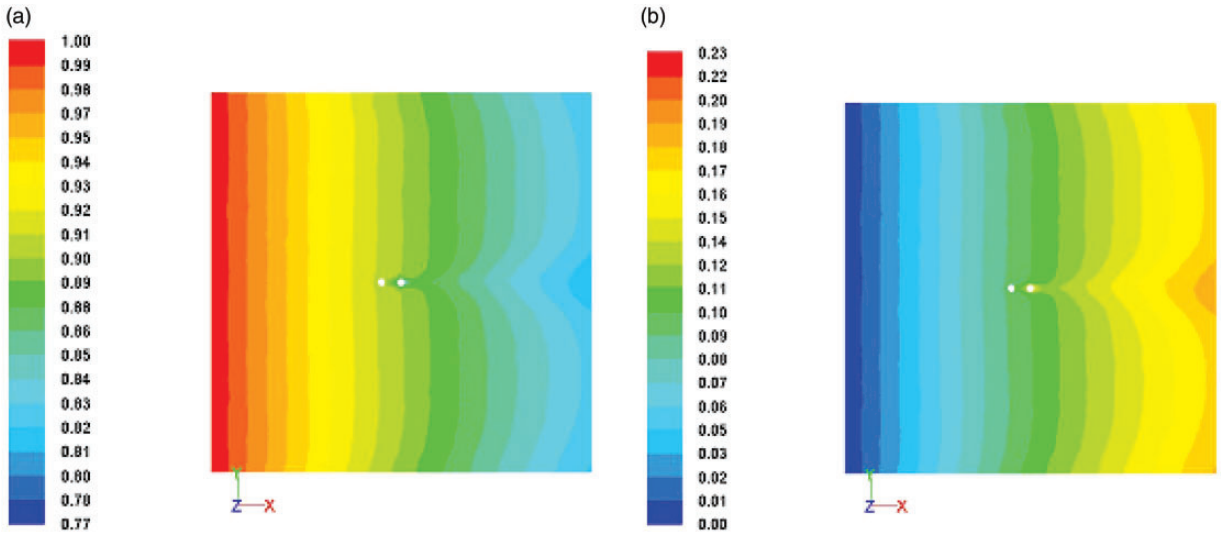

Figure 4. Contours of volume fraction of water and steam when $Re = 200$ and gap = 1.5 D: (a) water, (b) steam.

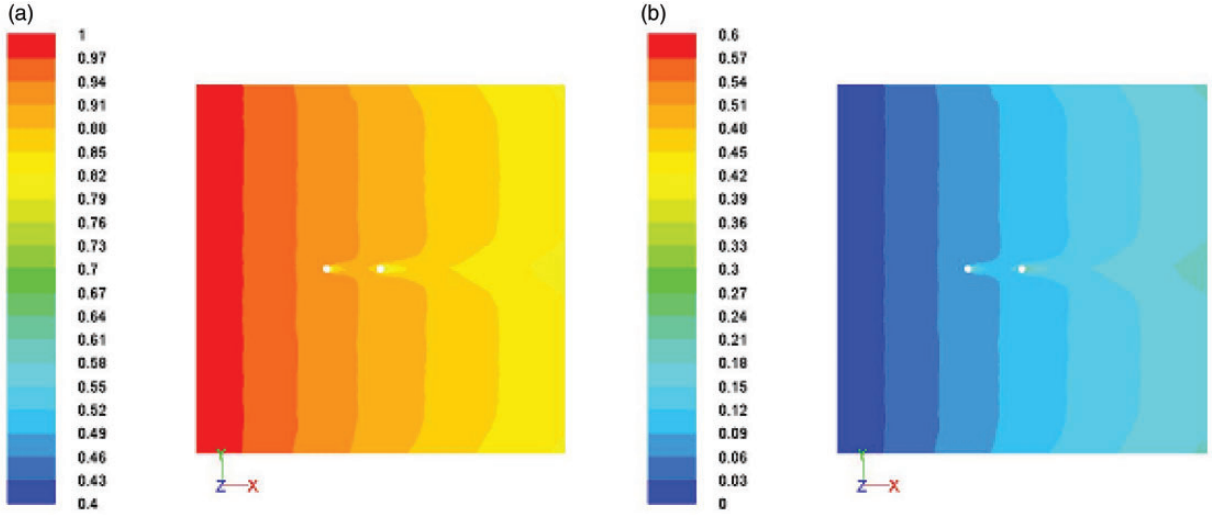

Figure 5. Contours of volume fraction of water and steam when $Re = 200$ and gap = 6 D: (a) water (b) steam.

surface heat transfer coefficients, where q is amount of heat transferred (heat flux, W/m^2), h is heat transfer coefficient (W/m^2.K), and ΔT is the temperature difference between the solid surface and surround fluid area, K.

Some of the results reported herein include the phase change and the corresponding volume fractions of two phases of the fluid.

Effect of the change of Reynolds number of flow

From Figures 4(a) and (b) and Figures 5(a) and (b), it is observed that, for $Re = 200$, the volume fraction of water for two spacing (1.5 D and 6 D) differs significantly. The same is true for the volume fraction of steam.

From Figures 6(a) and (b) and Figures 7(a) and (b), it is observed that, for $Re = 150{,}000$, the volume fraction of water for two spacings (1.5 D and 6 D) has almost the same value. The same is true for the volume fraction of steam.

The possible reason for such an observation in the case of $Re = 200$ could be the availability of more heat flux to water while it is flowing across two cylinders kept at 1.5 D. The volume fraction of water is reducing faster, whereas the volume fraction of steam is increasing when the flows are interacting and are extracting more heat from the both surfaces and lending it to the water present near to the surface.

The widening of the gap increases the scope of accumulating heat for a quicker conversion of water to steam. The maximum volume fraction of steam generated when the spacing is 1.5 D is increased by 61% compared with same value of steam when spacing is 6 D.

Another possibility is that the lower Re allows more resident time for water to be in touch with the heated

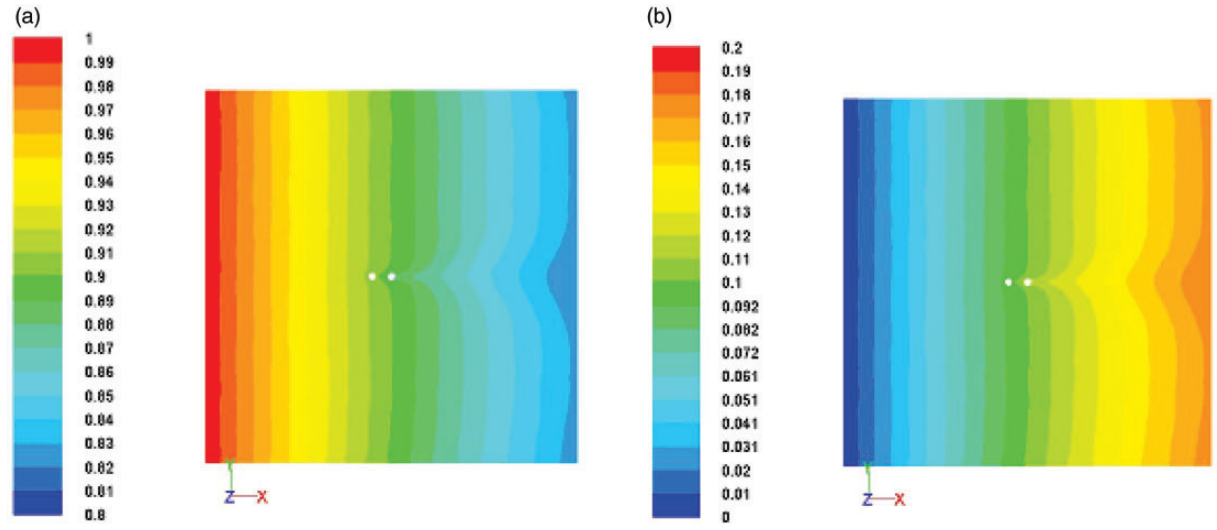

Figure 6. Contours of volume fraction of water and steam when $Re = 150{,}000$ and gap $= 1.5\ D$: (a) water, (b) steam.

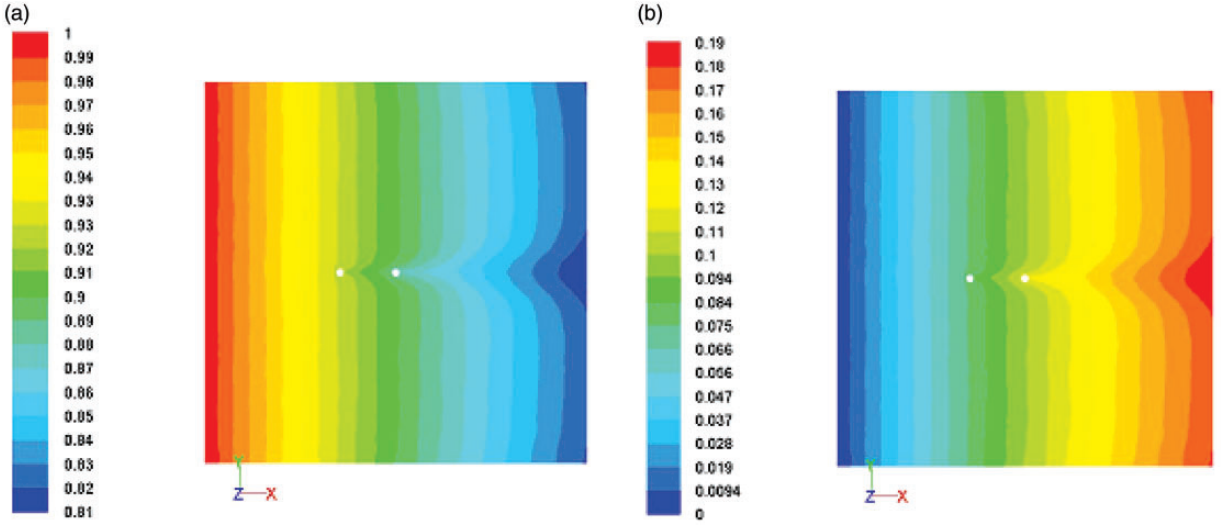

Figure 7. Contours of volume fraction of water and steam when $Re = 150{,}000$ and gap $= 6\ D$.

surface of the cylinder and hence the higher value of volume fraction of steam in the flow domain. The larger spacing alters the opportunity of absorbing more heat by water from the heated surface.

For $Re = 150{,}000$, it is observed from the contour plots in Figures 5(a) and (b) that the value of the volume fraction of steam for both the spacings (1.5 D and 6 D) shows a difference of 5%. So, this could be a poor heat and mass transfer phenomenon between the two phases and a weak heat convection (low heat transfer coefficient) from the heated solid surface to water. The turbulent flow ($Re = 150{,}000$) has decreased the opportunity for water to stay longer and closer to heated solid surface and it has resulted in a lower value of volume fraction of steam.

Figures 8 and 9 are the plots of the volume fraction of water versus position in a stream-wise direction and a plot of volume fraction of stream versus position in stream-wise direction when $Re = 200$ and 150,000 at spacing $= 1.5\ D$, respectively. The difference in the value of volume fraction is observed at locations $x = 0.07$ m, 0.08 m for the two different Reynolds numbers, respectively. These two locations are near the solid walls of the cylinders. The lower value of volume fraction for $Re = 200$ and the higher value of volume fraction for $Re = 150{,}000$ are justifying the logic that more heat transfer has occurred at $Re = 200$ and hence more steam is formed (higher volume fraction of steam at lower Re).

Figures 10 and 11 are the plots of the volume fraction of water versus position in a stream-wise direction

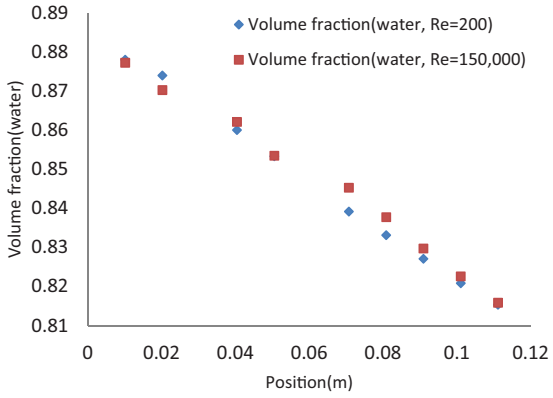

Figure 8. Plot of volume fraction of water versus position in stream-wise direction when $Re = 200$ and $Re = 150{,}000$ at spacing = 1.5 D.

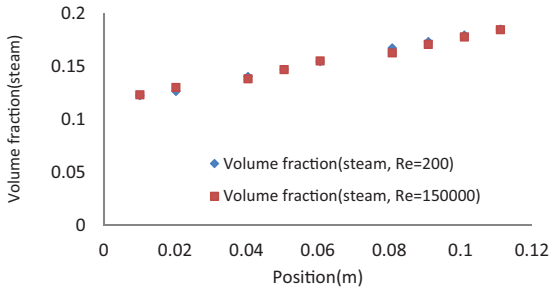

Figure 9. Plot of volume fraction of stream versus position in stream-wise direction when $Re = 200$ and $Re = 150{,}000$ at spacing = 1.5 D.

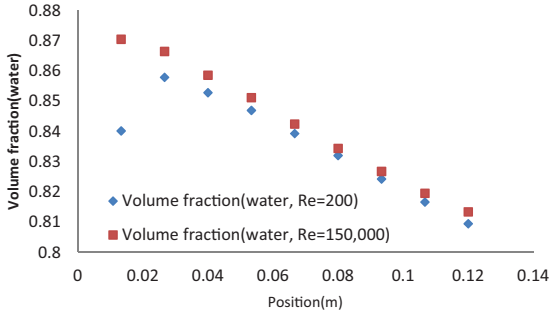

Figure 10. Plot of volume fraction of water versus position in stream-wise direction when $Re = 200$ and $Re = 150{,}000$ at spacing = 6 D.

and a plot of volume fraction of stream versus position in a stream-wise direction when $Re = 200$ and 150,000 at spacing = 6 D, respectively. The difference in the value of volume fraction is observed at all locations for the two different Reynolds numbers. The higher value of volume fraction for $Re = 200$ and lower value of volume fraction for $Re = 150{,}000$ are justifying the logic that more heat transfer has occurred at $Re = 200$ and hence more steam is formed (higher volume fraction of steam at lower Re).

Although the focus of the study is to observe the effect of Re and spacing on the phase change phenomenon, the flow field in wake region of downstream cylinder (Cylinder 2) has also been of special interest during the study and, hence, a few plots have been presented in this paper. The wake region behind the downstream cylinder (Cylinder 2) for spacing of 1.5 D is affected by both the heating of the surface and spacing between the two cylinders. Figure 12(a) depicts streamlines over an isolated circular cylinder where the flow is 2D and $Re = 200$ and Figure 12(b) shows streamlines in the wake zone for an isolated circular cylinder where flow is 3D and $Re = 200$. The flow fields in the wake regions are different. The flow field shown in Figure 12(b) is more chaotic than that in Figure 12(a), where the region seems to be predictable and recirculation area is distinct. The study was extended to observe the flow field in the case of a two-cylinder arrangement. One case (spacing = 1.5 D) has been presented as an illustration here in this paper to understand the nature of flow filed in the wake region of downstream cylinder. The wake region gets affected by the presence of an upstream cylinder which is displayed in Figure 13. The higher value of Re (here it is 150,000) assists the flow to diminish the larger wake region that is formed in the case of lower Re (it is 200), and the 3D effect along with heat flux from the surfaces of cylinders varies the flow field variables significantly. Figure 14 is a superimposed plot that shows the distribution of mean x-velocity down in the wake region of Cylinder 2. The low negative values of velocity and the direction of stream lines confirm that the reverse flow is quite evident in the wake area.

Conclusion

In this paper, the effect of phase change of water flowing across two heated circular cylinders in a tandem arrangement was studied at change in the Reynolds number. The Eulerian model was used during simulation to capture the data. First our results were verified with results mentioned in literature and then further data analysis was made for present conditions. It was observed that when the spacing is less, that is 1.5 D, the heat generated from the walls is more and hence water receives more heat from the walls. This contributes to a higher volume fraction for steam (around 54%) than that generated when the spacing is 6 D. The other finding from the solution of the above problem is that when the two cylinders are closer to each other (spacing is 1.5 D or interacting through flows) the heat transfer coefficient is almost 35% higher than that generated when the spacing is 6 D. To understand the interacting and non-interacting flows when two cylinders are kept in tandem, U^+values for the 1.5 D spacing are influenced

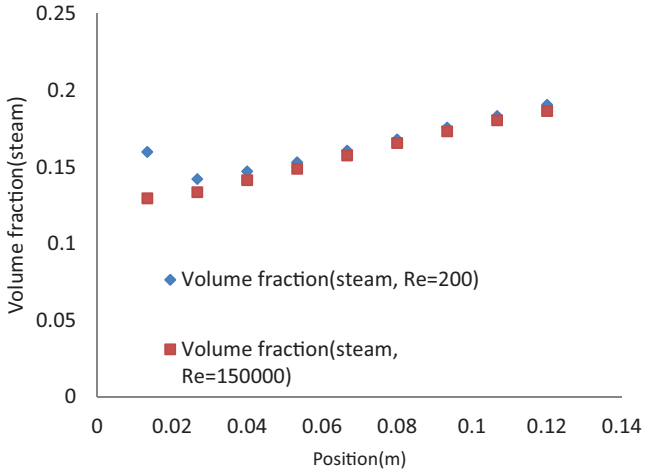

Figure 11. Plot of volume fraction of steam versus position in stream-wise direction when $Re = 200$ and $Re = 150{,}000$ at spacing $= 6\,D$.

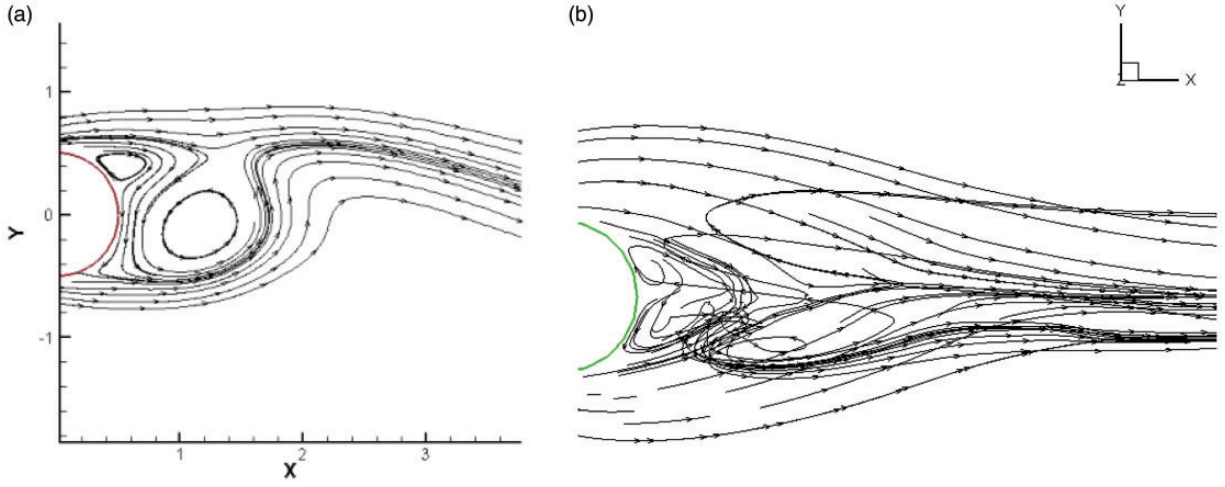

Figure 12. (a) Streamlines in the wake of a single cylinder (2D and $Re = 200$, validation case). (b) Stream lines in the wake of a single cylinder (3D and $Re = 200$, validation case).

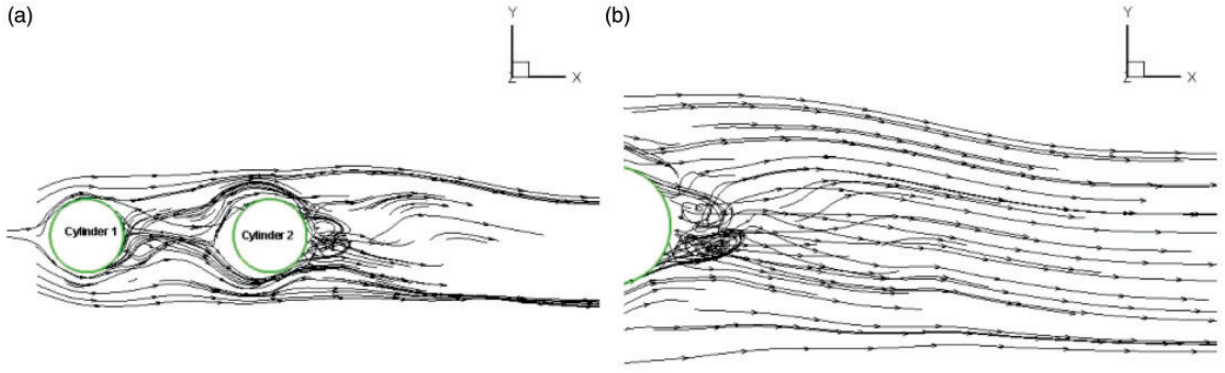

Figure 13. (a) Stream lines over the two cylinders (spacing $= 1.5\,D$, $Re = 150{,}000$). (b) Stream lines in the wake region of the downstream cylinder. (spacing $= 1.5\,D$, $Re = 150{,}000$).

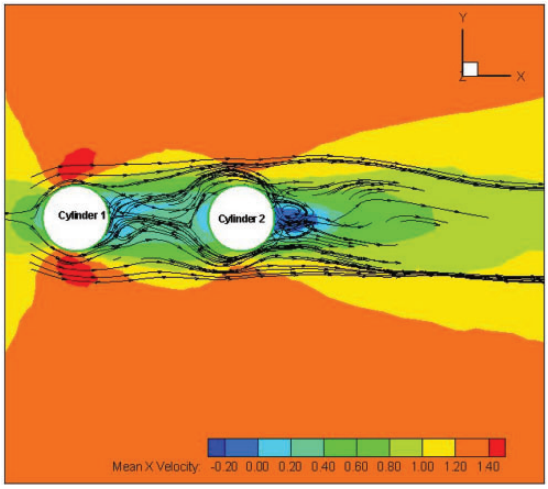

Figure 14. An illustrative and superimposed plot for stream lines and contours of mean *x*-velocity over the two cylinders (Cylinder 1 and Cylinder 2) for spacing = 1.5 *D* and *Re* = 150,000.

by the closeness of the two cylinders (hence flows are interacting), whereas the values of U^+ remain steady (particularly linear inside the domain covering spacing and hence flows are mostly non-interacting) for 6 *D* spacing.

The flow filed of the wake region of the downstream cylinder is affected by the spacing between Cylinder 1 and 2, *Re* of the flow, 3D of the flow, and the heat flux from the Cylinder 2. The mass, momentum, and heat transfer mechanisms are unidirectional in nature and hence they transfer from Phase 1 to Phase 2.

Declaration of Conflicting Interests

The author(s) declared no potential conflicts of interest with respect to the research, authorship, and/or publication of this article.

Funding

The author(s) received no financial support for the research, authorship, and/or publication of this article.

References

1. Zdravkovich MM. *Flow around circular cylinders, volume 1: fundamentals*. London: Oxford University Press, 1997.
2. Zdravkovich MM. *Flow around circular cylinders, volume 1: fundamentals*. London: Oxford University Press, 2003.
3. Mittal S, Kumar V and Raghuvanshi A. Unsteady incompressible flows past two cylinders in tandem and staggered arrangements. *Int J Numer Meth Fluids* 1997; 25: 1315–1344.
4. Meneghini JR, Saltara F, Siqueira CLR, et al. Numerical simulation of flow interference between two circular cylinders in tandem and side-by-side arrangements. *J Fluids Struct* 2001; 15: 327–350.
5. Ljungkrona L, Norberg C and Sundén B. Free-stream turbulence and tube spacing effects on surface pressure fluctuations for two tubes in an in-line arrangement. *J Fluid Struct* 1991; 5: 701–727.
6. Zhang H and Melbourne WH. Interference between two circular cylinders in tandem in turbulent flow. *J Wind Eng Ind Hydrodyn* 1992; 41: 589–600.
7. Bearmann PW and Wadcock AJ. The interaction between a pair of circular cylinders normal to a stream. *J Fluids Mech* 1973; 61: 499–511.
8. Liu K, Ma Dong-jun and Sun De-jun. Wake patterns of flow past a pair of circular cylinders in side by-side arrangements at low Reynolds numbers. *J Hydrodyn Ser B* 2007; 19: 690–697.
9. Ryu S, Lee SB and Lee BH. Estimation of hydrodynamic coefficients for flow around cylinders in side-by-side arrangement with variation in separation gap. *J Ocean Eng* 2009; 36: 672–680.
10. Mahir N and Altac Z. Numerical investigation of convective heat transfer in unsteady flow past two cylinders in tandem arrangements. *Int J Heat Fluid Flow* 2008; 29: 1309–1318.
11. Singha S and Sinhamahapatra KP. High resolution numerical simulation of low Reynolds number incompressible flow about two cylinders in tandem. *J Fluid Eng ASME* 2010; 132: 011101.
12. Ding H, Shu C and Yeo KS. Numerical simulation of flows around two circular cylinders by mesh-free least square-based finite difference methods. *Int J Numer Meth Fluids* 2007; 53: 305–332.
13. Kitagawa T and Ohta H. Numerical investigation on flow around circular cylinders in tandem arrangement at a subcritical Reynolds number. *J Fluid Struct* 2008; 24: 680–699.
14. Deng J, Ren An-lu and Chen Wen-qu. Numerical simulation of flow-induced vibration on two circular cylinders in tandem arrangement. *J Hydrodyn Ser B* 2005; 17: 660–666.
15. Moriya M, Alam M and Takai K. Fluctuating fluid forces of two circular cylinders in tandem arrangement at close spacing. *Transac Jpn Soc Mech Eng* 2002; 68: 1400–1406.
16. Zdravkovich MM. Review of flow interference between two circular cylinders in various arrangements. *J Fluids Eng* 1977; 37: 993–1010.
17. Ming-Ming L, et al. Re-examination of laminar flow over twin circular cylinders in tandem arrangement. *Fluid Dyn Res* 2014; 48: 1–21.
18. Drew DA and Lahey RT. *In particulate two-phase flow*. Boston: Butterworth-Heinemann, 1993, pp.509–566.
19. Rajani BN, Kandaswamy A and Sekhar M. Numerical simulation of laminar flow past a circular cylinder. *Appl Math Model* 2009; 33: 1228–1247.
20. Wang ZL, Fun JR and Cen K. Immersed boundary method for the simulation of 2D viscous flow based on vorticity-velocity formulations. *J Comput Phys* 2009; 228: 1504–1520.
21. Zhang X, Ni SZ and He GW. A pressure correction method and its applications on an unstructured chimera grid. *Comput Fluids* 2008; 37: 993–1010.

22. Linnick MN and Fasel HF. A high-order immersed interface method for simulating unsteady incompressible flows on irregular domains. *J Comput Phys* 2005; 204: 157–192.
23. Farrani T, Tan M and Price WG. A cell boundary element method applied to laminar vortex shedding from circular cylinder. *Comput Fluids* 2001; 30: 211–236.
24. He JW, Glowinski R, Motcalfe R, et al. Active control and drag optimization for flow past a circular cylinder. *J Comput Phys* 2000; 163: 83–117.
25. Henderson RD. Details of the drag curve near the onset of vortex shedding. *Phys Fluids* 1995; 7: 2102–2104.
26. Schiller L and Naumann Z. A drag coefficient correlation. Z Ver. Deutsch. *Ing* 1935; 77: 318.

Appendix

Notation

C_{D}	drag coefficient, dimensionless
C_{L}	lift coefficient, dimensionless
d_p	diameter of the bubbles or droplet of phase ***p***, m
$\frac{d_Q}{d_t}$	phase material time derivative
D	diameter of the cylinder, m
$\vec{F}_{lift/q}$	lift force for phase q, N
$\vec{F}_q$	external body force for phase q, N
$\vec{F}_{vm/q}$	virtual mass
$G_{\mathrm{k,m}}$	production of turbulence kinetic energy
h_{pq}	interphase enthalpy, Joule
h_p	specific enthalpy of the ***q***th phase, Joule/kg
k	turbulent kinetic energy, $\mathrm{m}^2/\mathrm{s}^2$
K_{pq}	interphase momentum exchange coefficient
L	length of the flow domain in the axial direction, m
p	pressure, Pa
$\vec{q}_q$	heat flux, $\mathrm{Watt/m}^2$
Re	Reynolds number ($\rho U - D/\mu$), dimensionless
$\vec{R}_{pq}$	interaction force between phases
St	Strouhal number, dimensionless
t	time, s
T	temperature, K
u	x-velocity, m/s
U	velocity of the fluid, m/s
$U_{\_}$	free stream velocity of the fluid at the inlet, m/s
v	y-velocity, m/s
V_q	volume of the phase q, m^3
x	stream-wise coordinate, m
y	transverse coordinate, m
α_q	phasic volume fraction of the phase q, dimensionless
ϵ	rate of dissipation rate of turbulent kinetic energy, $\mathrm{m}^2/\mathrm{s}^3$
λ_q	bulk viscosity of phase q
μ	dynamic viscosity of fluid, kg/m-s
$\mu_{t,m}$	turbulent viscosity of mixture, kg/m-s
μ_q	shear viscosity of phase q
ρ	density, $\mathrm{kg/m}^3$
$\widehat{p}_q$	effective density of phase q
ρ_q	physical density of phase q, $\mathrm{kg/m}^3$
τ_p	''particulate relaxation'' time
$\vec{v}_q$	velocity of phase q, m/s